Septin-Mediated Plant Cell Invasion by the Rice Blast Fungus, *Magnaporthe oryzae*

Yasin F. Dagdas *et al.*

Science **336**, 1590 (2012);
DOI: 10.1126/science.1222934

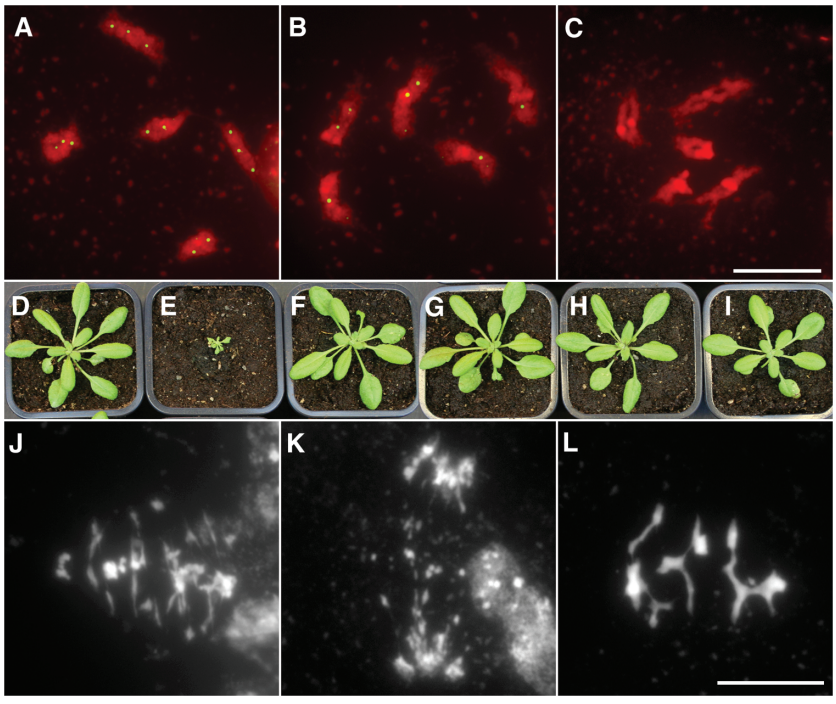

Fig. 4. *fancm* extra COs are MUS81 dependent. (**A** to **C**) MLH1 immunolocalization at diakinesis. (A) Wild type. (B) *fancm-1.* (C) *fancm-1 zip4*. (**D** to **I**) Analysis of the *fancm mus81* synthetic growth defect. (D) Wild type. (E) *fancm mus81*. (F) *fancm mus81 rad51.* (G) *fancm*. (H) *mus81.* (I) *rad51*. (**J** to **L**) Meiotic chromosome spreads. (J) *fancm-1 zip4 mus81* with chromosome fragmentation at the metaphase I to anaphase I transition. (K and L) *fancm-1 mus81* showing chromosome fragmentation at anaphase I and five bivalent-like structures at metaphase I, respectively. Scale bars: 10 μm.

of ZMM-dependent COs is indifferent to the defective MUS81 FANCM pathways.

In mitotic cells, budding and fission yeast orthologs of the FANCM helicase—Mph1 and Fml1, respectively—have been shown to unwind displacement loops (D loops) in NCO pathways and to be somatic CO suppressors (*13*, *14*). The biochemical properties of FANCM helicases are likely similar at mitosis and meiosis. We suggest that FANCM processes meiotic DSB repair intermediates, possibly D loops, driving them toward NCO resolution (or sister chromatid events) (fig. S1). In the absence of FANCM, MUS81 repairs these intermediates as interference-insensitive COs, whereas ZMMs cannot process these intermediates as COs. This implies that recombination intermediates on which FANCM can act are distinct from the intermediates that ZMMs converts to COs, supporting an early irreversible channeling of intermediates toward the ZMM or MUS81 pathways (*9*). To date, only two other meiotic anti-CO factors have been described (*1*): R-TEL in *Caenorhabditis elegans* (*15*) and Sgs1 in budding yeast (*16*, *17*). Thus, anti-CO factors identified so far are helicases, raising the possibility that different helicases are used in various organisms to prevent excessive COs. Additionally, our findings show that, although most eukaryotes have only one to three COs per chromosome on average, CO number can be largely increased without obvious negative phenotypic effects, suggesting that COs are naturally constrained below their possible maximum. This finding supports the idea that crossover frequency is maintained by natural selection at a specific equilibrium between the long-term advantages and costs of recombination (*18*). Finally, the hyperrecombination provoked by *fancm* mutation could be of great interest for crop improvement, which relies on the production of new allele combinations through meiotic recombination whose frequency is a limiting factor (*19*).

References and Notes

1. J. L. Youds, S. J. Boulton, *J. Cell Sci.* **124**, 501 (2011).
2. L. E. Berchowitz, G. P. Copenhaver, *Curr. Genomics* **11**, 91 (2010).
3. L. Chelysheva *et al.*, *PLoS Genet.* **3**, e83 (2007).
4. M. C. Whitby, *DNA Repair (Amst.)* **9**, 224 (2010).
5. A. R. Meetei *et al.*, *Nat. Genet.* **37**, 958 (2005).
6. L. E. Berchowitz, G. P. Copenhaver, *Nat. Protoc.* **3**, 41 (2008).
7. A. Malkova *et al.*, *Genetics* **168**, 49 (2004).
8. L. Chelysheva *et al.*, *Cytogenet. Genome Res.* **129**, 143 (2010).
9. G. V. Börner, N. Kleckner, N. Hunter, *Cell* **117**, 29 (2004).
10. F. W. Stahl, *Genetics* **179**, 701 (2008).
11. J. D. Higgins, E. F. Buckling, F. C. H. Franklin, G. H. Jones, *Plant J.* **54**, 152 (2008).
12. L. E. Berchowitz, K. E. Francis, A. L. Bey, G. P. Copenhaver, *PLoS Genet.* **3**, e132 (2007).
13. W. Sun *et al.*, *Mol. Cell* **32**, 118 (2008).
14. R. Prakash *et al.*, *Genes Dev.* **23**, 67 (2009).
15. J. L. Youds *et al.*, *Science* **327**, 1254 (2010).
16. S. D. Oh *et al.*, *Cell* **130**, 259 (2007).
17. A. De Muyt *et al.*, *Mol. Cell* **46**, 43 (2012).
18. L. Hadany, J. M. Comeron, *Ann. N.Y. Acad. Sci.* **1133**, 26 (2008).
19. E. Wijnker, H. de Jong, *Trends Plant Sci.* **13**, 640 (2008).
20. D. D. Perkins, *Genetics* **34**, 607 (1949).

Acknowledgments: R.M. and J.L.S. thank the EU-FP7 program (Meiosys-KBBE-2009-222883), and G.P.C. thanks the NSF (MCB-1121563) for financial support. We thank V. Borde, M. Grelon, C. Mézard, F. Nogué, A. Demuyt, and O. Loudet for critical reading of the manuscript and helpful discussions. A provisional patent application based on the work has been filed by INRA.

Supplementary Materials

www.sciencemag.org/cgi/content/full/336/6088/1588/DC1
Materials and Methods
Figs. S1 to S8
Tables S1 to S5
References (*21*–*30*)

10 February 2012; accepted 17 April 2012
10.1126/science.1220381

Septin-Mediated Plant Cell Invasion by the Rice Blast Fungus, *Magnaporthe oryzae*

Yasin F. Dagdas,[1] Kae Yoshino,[1,2] Gulay Dagdas,[1] Lauren S. Ryder,[1] Ewa Bielska,[1] Gero Steinberg,[1] Nicholas J. Talbot[1]*

To cause rice blast disease, the fungus *Magnaporthe oryzae* develops a pressurized dome-shaped cell called an appressorium, which physically ruptures the leaf cuticle to gain entry to plant tissue. Here, we report that a toroidal F-actin network assembles in the appressorium by means of four septin guanosine triphosphatases, which polymerize into a dynamic, hetero-oligomeric ring. Septins scaffold F-actin, via the ezrin-radixin-moesin protein Tea1, and phosphatidylinositide interactions at the appressorium plasma membrane. The septin ring assembles in a Cdc42- and Chm1-dependent manner and forms a diffusion barrier to localize the inverse-bin-amphiphysin-RVS–domain protein Rvs167 and the Wiskott-Aldrich syndrome protein Las17 at the point of penetration. Septins thereby provide the cortical rigidity and membrane curvature necessary for protrusion of a rigid penetration peg to breach the leaf surface.

Rice blast is the most devastating disease of cultivated rice and a constant threat to global food security. Each year up to 30% of the rice harvest is lost to blast disease—enough grain to feed 60 million people—and finding an effective way to control rice blast is therefore a

priority. To infect rice leaves, *Magnaporthe oryzae* develops a special infection structure called an appressorium (Fig. 1), which generates turgor of up to 8.0 MPa (equivalent to 40 times that of a car tire) and translates this extreme pressure into physical force to break the leaf surface. Appressorium turgor is generated by rapid influx of water into the cell against a concentration gradient of glycerol, maintained in the appressorium by a specialized, melanin-rich cell wall (*1*). Turgor is translated into physical force and applied to the leaf surface by a narrow penetration peg that mechanically ruptures the tough leaf cuticle (*2*, *3*). The cellular mechanism by which an appressorium breaches the cuticle is not known.

We set out to investigate how the appressorium causes plant infection. We first carried out live-cell imaging of the actin cytoskeleton during appressorium maturation by expressing the actin-binding protein gene fusion, LifeAct-RFP (where RFP is red fluorescent protein) (*4*), in *M. oryzae*.

[1]School of Biosciences, University of Exeter, Geoffrey Pope Building, Exeter EX4 4QG, UK. [2]Division of Applied Biosciences, Graduate School of Agriculture, Kyoto University, Sakyo-ku, Kyoto 606-8502, Japan.

*To whom correspondence should be addressed. E-mail: n.j.talbot@exeter.ac.uk

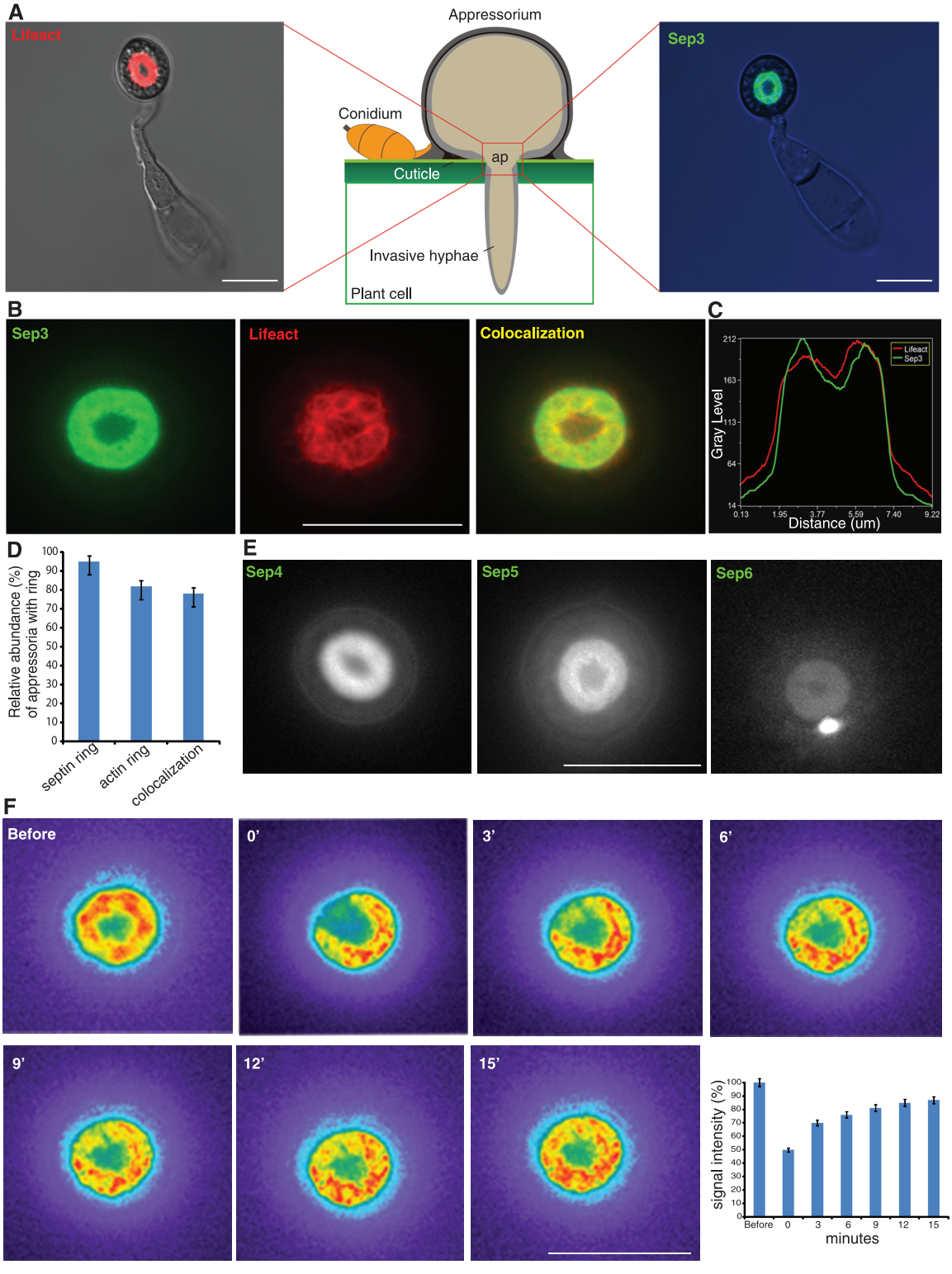

Fig. 1. A toroidal-shaped F-actin network and septin ring assemble at the appressorium pore in *M. oryzae*. (**A**) Cellular localization of LifeAct-RFP and Sep3-GFP visualized by laser confocal and laser excitation epifluorescence microscopy, respectively. ap indicates appressorium pore. (**B**) Sep3-GFP and LifeAct-RFP colocalization in the appressorium. (**C**) Linescan graph consistent with colocalization of the septin ring and F-actin network. (**D**) Bar charts showing septin ring and F-actin colocalization (mean ± SD, three experiments, n = 300). (**E**) Sep3-GFP, Sep4-GFP, Sep5-GFP, and Sep6-GFP form a ring at the appressorium pore. Sep6 also forms a distinct punctum. (**F**) Recovery of Sep3-GFP ring after partial photobleaching, with 87% recovery in fluorescence after 15 min (mean ± SD, three experiments). Scale bars indicate 10 μm.

This revealed an extensive toroidal F-actin network at the base of the infection cell surrounding the appressorium pore (Fig. 1A), a circular region that marks the point at which the penetration peg emerges to rupture the leaf cuticle (*2*). The appressorium pore initially lacks a cell wall, and the fungal plasma membrane makes direct contact with the rice leaf surface (*2*). Then, as the appressorium inflates to full turgor (with a mean diameter of 8.0 μm), a pore wall overlay develops, and a narrow (780-nm mean diameter) penetration peg emerges. Assembly of an F-actin network during appressorium turgor generation, just before plant infection, suggests that specific reorientation of the F-actin cytoskeleton takes place at the base of the appressorium to facilitate plant infection (*2*). To investigate how actin is organized at this location, we decided to investigate the septin gene family in *M. oryzae*. Septins are small morphogenetic guanosine triphosphatases (GTPases); conserved from yeast to humans (*5*, *6*); and involved in cytokinesis, polarity determination, and secretion (*7*, *8*). Importantly, septins are thought to reorient and reorganize the cytoskeleton to determine cell shape (*9*–*12*) and act as partitioning diffusion barriers to recruit and maintain specific proteins at discrete subcellular locations (*9*, *10*). We identified a family of five septin genes in *M. oryzae*, four of which showed similarity to core septins identified in the budding yeast *Saccharomyces cerevisiae* (Cdc3, Cdc10, Cd11, and Cdc12) (*9*). Sep3 showed 47% amino acid identity to Cdc3, Sep4 showed 55% identity to Cdc10, Sep5 showed 45% identity to Cdc11, and Sep6 showed 57% identity to Cdc12. We expressed the *M. oryzae* genes in temperature-sensitive *S. cerevisiae* septin mutants that show defects in cell division and in all cases observed complementation of the cell separation defect consistent with the *M. oryzae* proteins acting as functional septins (fig. S1). Next, we expressed Sep3-GFP, Sep4-GFP, Sep5-GFP, and Sep6-GFP (where GFP is green fluorescent protein) gene fusions in *M. oryzae*, and each septin formed a 5.9-μm ring that colocalized with the F-actin network at the appressorium pore (Fig. 1, A and D, and movie S1). In the case of Sep6-GFP, we also observed an additional bright punctate structure consistently associated with the appressorium septin ring (Fig. 1D). *M. oryzae* septins formed a wider range of structures in hyphae and during invasive growth, including bars, gauzes, collars, and rings (figs. S2 and S3). As expected, they also formed rings at sites of septation (*10*), such as the neck of nascent appressoria (fig. S2). To understand the nature of the septin ring, we investigated fluorescence recovery after partial photobleaching. We found 87% recovery of fluorescence after 15 min, consistent with the appressorium septin ring being a dynamic structure (Fig. 1F). We then carried out targeted gene deletions to produce isogenic mutants lacking *SEP3*, *SEP4*, *SEP5*, or *SEP6* (fig. S4). Septin null mutants showed mislocalization of the remaining septin-GFPs (fig. S5). Core *M. oryzae* septins therefore act cooperatively to form hetero-oligomers, which assemble into the large ring surrounding the appressorium pore. Consistent with this idea, coimmunoprecipitation experi-

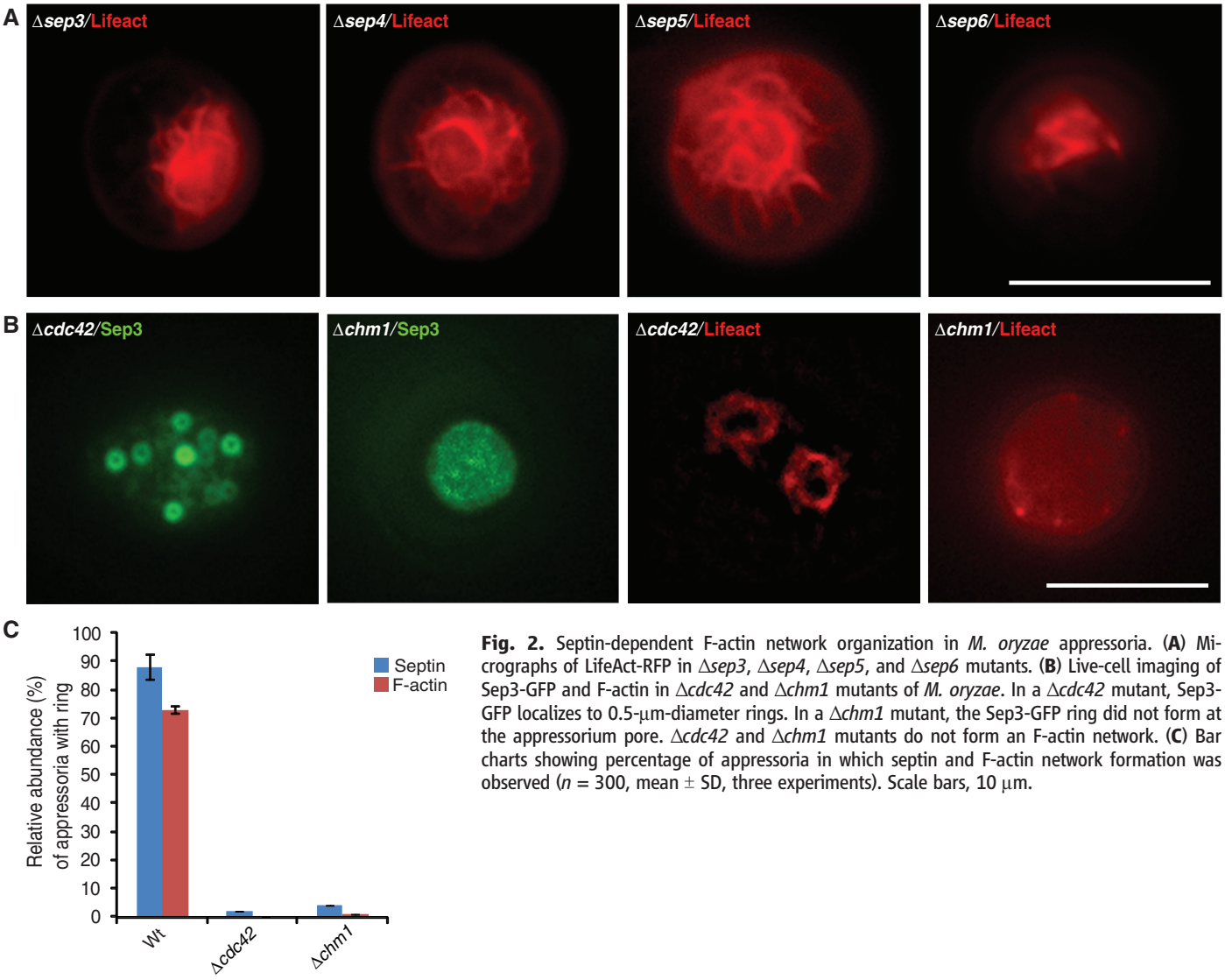

Fig. 2. Septin-dependent F-actin network organization in *M. oryzae* appressoria. (**A**) Micrographs of LifeAct-RFP in Δ*sep3*, Δ*sep4*, Δ*sep5*, and Δ*sep6* mutants. (**B**) Live-cell imaging of Sep3-GFP and F-actin in Δ*cdc42* and Δ*chm1* mutants of *M. oryzae*. In a Δ*cdc42* mutant, Sep3-GFP localizes to 0.5-μm-diameter rings. In a Δ*chm1* mutant, the Sep3-GFP ring did not form at the appressorium pore. Δ*cdc42* and Δ*chm1* mutants do not form an F-actin network. (**C**) Bar charts showing percentage of appressoria in which septin and F-actin network formation was observed (n = 300, mean ± SD, three experiments). Scale bars, 10 μm.

ments using Sep5-GFP identified Sep3, Sep4, and Sep6 interactions as well as physical interaction with actin, tubulins, and the Lte1 cell cycle control protein (*11*) (table S1). *M. oryzae* septin mutants showed a number of developmental phenotypes (fig. S6). Multiple rounds of nuclear division, for instance, took place during appressorium development in septin mutants (fig. S7, A and B) compared with a single round of mitosis and autophagy-associated cell death, which normally occurs in *M. oryzae* (*12*, *13*). Septins took part in cytokinesis within hyphae (*7*–*10*), and localization of myosin II and myosin light chain to the septum, which separates the germ tube and appressorium (*10*), required septins (fig. S7, C and D).

We next decided to investigate the effect of deleting *M. oryzae* septin genes on actin organization and found that the appressorium F-actin network was disorganized in Δ*sep3*, Δ*sep4*, Δ*sep5*, and Δ*sep6* mutants (Fig. 2A). We reasoned that F-actin, scaffolded by septins, might therefore provide cortical rigidity before peg emergence in a manner analogous to a yeast bud, where assembly of F-actin cables requires Cdc42 and the formins Bni1 and Bnr1 (*14*–*16*). To test this idea, we investigated F-actin and septin localization in a *M. oryzae* Δ*cdc42* mutant (Fig. 2). We observed many aberrant, ~0.5-μm-diameter Sep3-GFP rings in a Δ*cdc42* mutant but no central septin ring in the appressorium (Fig. 2, B and C). Similarly, targeted deletion of *M. oryzae CHM1* (*17*, *18*) prevented formation of either the septin or F-actin networks (Fig. 2, B and C). In yeast, Chm1 encodes a kinase that phosphorylates septins (*17*). Septin ring formation also required the cell integrity mitogen-activated protein kinase Mps1 (*19*) and the Mst12 transcription factor (*20*), which are necessary for appressorium function (fig. S8). Furthermore, we discovered that septin ring formation depends on cell cycle progression, which regulates appressorium development in *M. oryzae* (*12*) (fig. S9). Taken together, we conclude that septin ring assembly is necessary to scaffold F-actin as a toroidal network at the base of the appressorium before plant infection.

To test whether septin-dependent assembly of the F-actin network is essential for rice blast disease, we inoculated a susceptible rice cultivar with each septin null mutant and scored disease symptoms. Septin mutants were nonpathogenic, causing either no symptoms at all (Δ*sep3*) or small necrotic flecks associated with abortive infection attempts that stimulate a rice defense response (Fig. 3, A and B). Transmission electron microscopy and live-cell imaging of rice leaf sheath infections by Δ*sep3* mutants confirmed the inability of appressoria from septin mutants to rupture plant cuticles efficiently (Fig. 3, C and D). All septin mutant phenotypes were complemented by reintroduction of either a wild-type allele or the corresponding septin-GFP fusion (fig. S10).

To understand the nature of the cortical F-actin network in appressoria, we decided to investigate plasma membrane linkages at the appressorium base. It has been suggested that some F-actin–plasma membrane linkages may occur via ezrin, radixin, moesin (ERM) proteins, which contain a C-terminal actin-binding domain and an N-terminal ERM domain that binds transmembrane proteins, such as integrins (*21*). We identified a putative ERM protein-encoding gene in *M. oryzae*, *TEA1* (which showed 61% identity to *S. pombe* Tea1), and found that Tea1-GFP localized as a punctate ring in the appressorium, colocated with the F-actin and septin networks (Fig. 4A and fig. S11B). By contrast, in a Δ*sep5* mutant, Tea1-GFP was mislocalized (Fig. 4A and fig. S11E). Phosphorylation of ERM proteins is potentiated by phosphatidylinositol (PtdIns)–4,5-bisphosphate binding (*22*). Yeast septins, for example, associate with PtdIns-4-phosphate and PtdIns-4,5-bisphosphate via an N-terminal polybasic domain (*23*, *24*). We identified the *M. oryzae* PtdIns-4-kinase–encoding gene, *STT4* (showing 53% identity to *S. cerevisiae STT4*), and the PtdIns-4-phosphate-5-kinase–encoding gene, *MSS4* (64% identity), and found that Stt4-GFP and Mss4-GFP localized to the appressorium pore, bounded by F-actin and the septin ring (Fig. 4B). To test

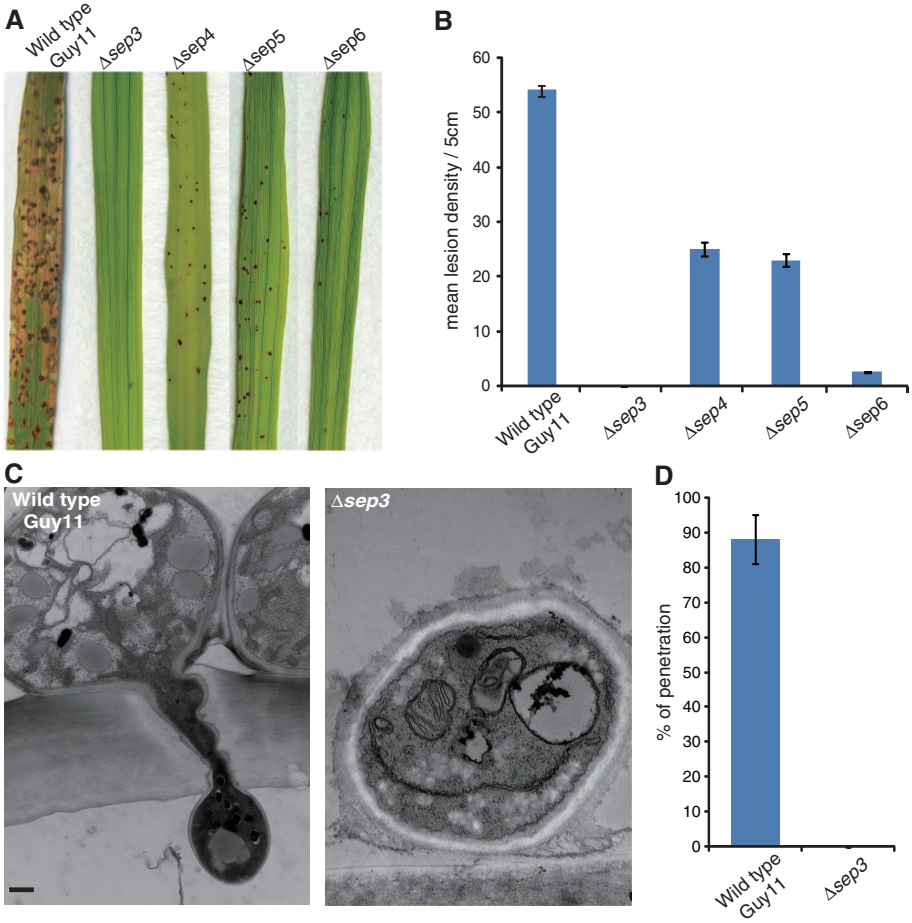

Fig. 3. *M. oryzae* septin mutants are unable to cause rice blast disease. (**A**) Targeted deletion of septin genes resulted in loss of pathogenicity on susceptible rice cultivar CO-39. The Δ*sep3* mutant caused no disease symptoms; Δ*sep4*, Δ*sep5*, and Δ*sep6* mutants elicited necrotic flecks because of abortive infection attempts. Septin mutants did not produce spreading disease lesions observed in the isogenic wild-type Guy11. (**B**) Bar chart shows frequency of disease lesions or necrotic flecks per 5 cm^2 of leaf surface (n = 30 plants) (mean ± SD, three experiments), reflecting frequency of penetration attempts. (**C**) Transmission electron micrographs of transverse section of wild-type (24 hours) and Δ*sep3* mutant appressoria (36 hours) during leaf infection. No penetration pegs were observed in Δ*sep3* mutants. Scale bar, 2 μm. (**D**) Bar chart showing frequency of rice epidermal cell rupture at 400 infection sites, 36 hours after conidial germination in wild type (Guy11) and Δ*sep3* mutants (mean ± SD, three experiments).

whether *M. oryzae* septins associated with membrane domains enriched in phosphoinositides, we deleted the N-terminal polybasic domain of *M. oryzae* Sep5 and expressed the resulting Sep5Δpb-GFP fusion protein in a Δ*sep5* mutant. The Sep5Δpb-GFP formed normal septin rings at hyphal septa or the neck of the nascent appressorium, demonstrating that stability of the septin was unaffected by deletion of the polybasic domain (Fig. 4C). However, the septin ring at the base of the appressorium did not form (Fig. 4C). We conclude that septin-PtdIns interactions and ERM protein-actin linkages occur at the appressorium pore. *M. oryzae* Chm1-GFP also localized to the appressorium pore (Fig. 4D and fig. S11, A and F), consistent with a role in septin phosphorylation (*25*).

We reasoned that, as well as scaffolding F-actin, the septin ring might also act as a diffusion barrier to constrain lateral diffusion of membrane-associated proteins involved in plant infection. Septin rings are known, for example, to act as diffusion barriers at the mother bud neck in *S. cerevisiae* (*26*, *27*). We decided to test whether *M. oryzae* septins affect distribution of proteins potentially involved in penetration peg development. Bin-amphiphysin-Rvs (BAR) domain proteins have been shown to form oligomeric scaffolds involved in membrane curvature (*28*). Whereas F-BAR proteins are well known to play roles in membrane invagination during endocytosis, the inverse BAR (I-BAR) proteins are involved in negative membrane curvature leading to cellular protrusions (*28*). Because emergence of a penetration hypha from the appressorium requires extreme negative membrane curvature (*2*, *29*), we decided to ask whether septins play a role in I-BAR protein localization. *M. oryzae* Rvs167 contains an I-BAR domain, showing 75% identity to *S. cerevisiae* Rvs167p. We found that Rvs167-GFP localized to the center of the appressorium pore, before penetration peg emergence. However, distribution of Rvs167-GFP was disrupted in a Δ*sep5* mutant (Fig. 4E and fig. S11, C and G). I-BAR proteins are proposed to link curved membrane structures to polymerization of cortical F-actin via nonspecific electrostatic interactions (*30*) mediated by Src homology 3 (SH3) domains of I-BAR proteins and components of the Wiskott-Aldrich syndrome protein (WASP)/WASP-family verprolin-homologous protein (WAVE) complex (*31*). We isolated a WASP/Arp2/3 complex component, Las17 (*32*), homologous to Las17p of *S. cerevisiae*. *M. oryzae* Las17-GFP localized to the base of the appressorium, bounded by the septin ring (Fig. 4F), whereas in a Δ*sep5* mutant Las17-GFP localization was disrupted, with the protein distributed diffusely in the cytoplasm and plasma membrane (Fig. 4F and fig. S11, D and H).

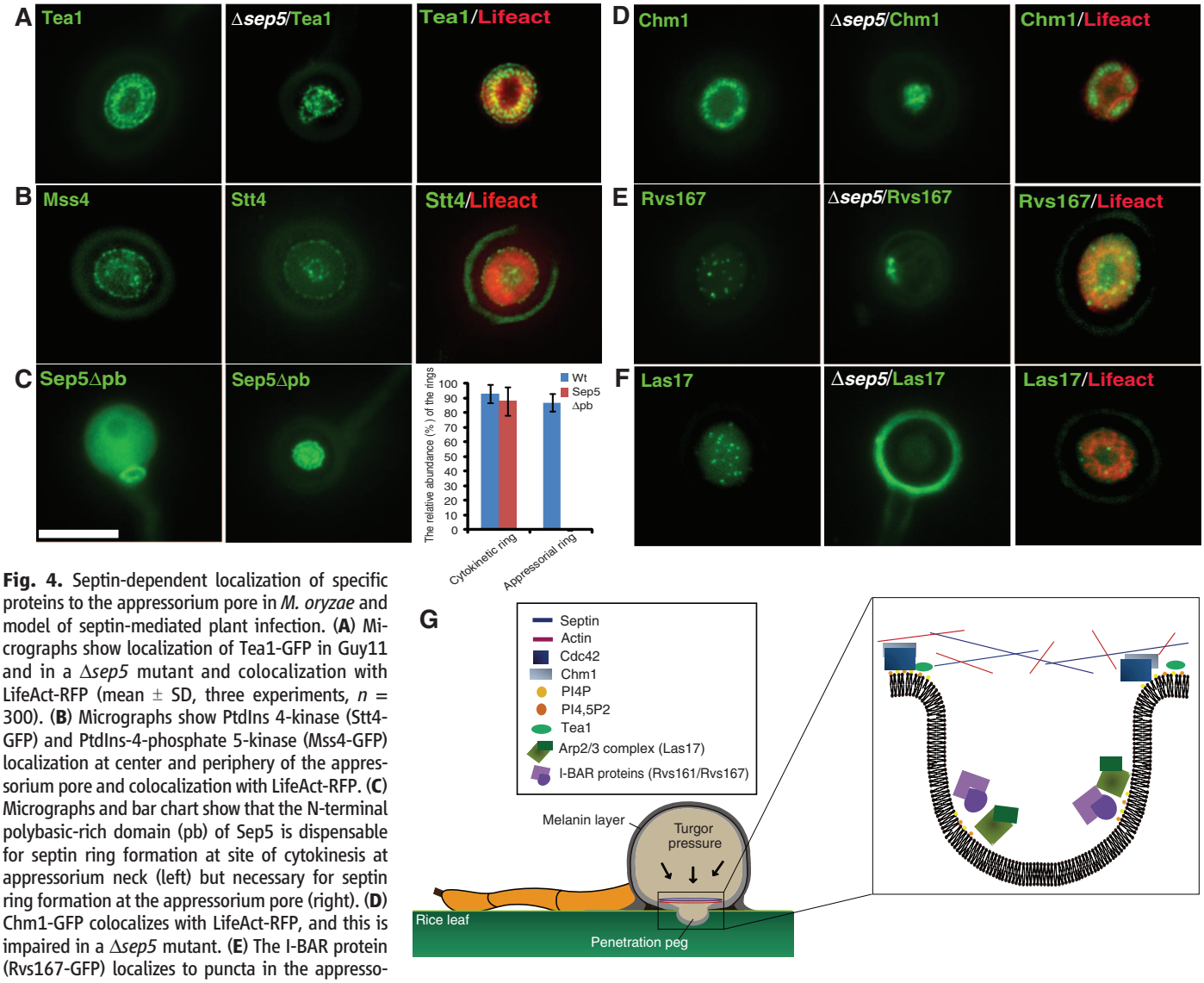

Fig. 4. Septin-dependent localization of specific proteins to the appressorium pore in *M. oryzae* and model of septin-mediated plant infection. (**A**) Micrographs show localization of Tea1-GFP in Guy11 and in a Δ*sep5* mutant and colocalization with LifeAct-RFP (mean ± SD, three experiments, n = 300). (**B**) Micrographs show PtdIns 4-kinase (Stt4-GFP) and PtdIns-4-phosphate 5-kinase (Mss4-GFP) localization at center and periphery of the appressorium pore and colocalization with LifeAct-RFP. (**C**) Micrographs and bar chart show that the N-terminal polybasic-rich domain (pb) of Sep5 is dispensable for septin ring formation at site of cytokinesis at appressorium neck (left) but necessary for septin ring formation at the appressorium pore (right). (**D**) Chm1-GFP colocalizes with LifeAct-RFP, and this is impaired in a Δ*sep5* mutant. (**E**) The I-BAR protein (Rvs167-GFP) localizes to puncta in the appressorium pore, and its organization is affected in a Δ*sep5* mutant. (**F**) Localization of the N-WASP protein (Las17-GFP), a component of the actin-polymerizing Arp2/3 complex, to the center of the appressorium pore septin ring and impairment of its localization in a Δ*sep5* mutant. Scale bar, 10 μm. (**G**) Model to show septin-mediated rice leaf infection by *M. oryzae*.

On the basis of the evidence presented in this report, we propose that appressoria of the rice blast fungus infect plants by using a septin-dependent mechanism summarized in Fig. 4G. In this model, isotropic expansion of the pressurized appressorium is directed into mechanical force at the base of the infection cell. This is dependent on assembly of an extensive toroidal F-actin network at the appressorium pore to provide cortical rigidity at the initially wall-less region of the appressorium. Septins organize the actin network, making direct phosphoinositide linkages to the plasma membrane and facilitating the action of ERM proteins, such as Tea1, which link cortical F-actin to the membrane. The septin ring also acts as a diffusion barrier to ensure localization of proteins, such as the Rvs167 I-BAR protein, and the WASP/WAVE complex involved in membrane curvature at the tip of the emerging penetration peg and F-actin polymerization (Fig. 4G). In this way, the rice blast fungus extends a rigid penetration peg that ruptures the leaf cuticle and invades the host plant tissue.

References and Notes

1. J. C. de Jong, B. J. McCormack, N. Smirnoff, N. J. Talbot, *Nature* **389**, 244 (1997).
2. T. M. Bourett, R. J. Howard, *Can. J. Bot.* **68**, 329 (1990).
3. C. Bechinger *et al.*, *Science* **285**, 1896 (1999).
4. A. Berepiki, A. Lichius, J. Y. Shoji, J. Tilsner, N. D. Read, *Eukaryot. Cell* **9**, 547 (2010).
5. A. S. Gladfelter, L. Kozubowski, T. R. Zyla, D. J. Lew, *J. Cell Sci.* **118**, 1617 (2005).
6. R. Lindsey, M. Momany, *Curr. Opin. Microbiol.* **9**, 559 (2006).
7. L. M. Douglas, F. J. Alvarez, C. McCreary, J. B. Konopka, *Eukaryot. Cell* **4**, 1503 (2005).
8. E. T. Spiliotis, W. J. Nelson, *J. Cell Sci.* **119**, 4 (2006).
9. L. H. Hartwell, *Exp. Cell Res.* **69**, 265 (1971).
10. D. G. Saunders, Y. F. Dagdas, N. J. Talbot, *Plant Cell* **22**, 2417 (2010).
11. G. A. Castillon *et al.*, *Curr. Biol.* **13**, 654 (2003).
12. D. G. Saunders, S. J. Aves, N. J. Talbot, *Plant Cell* **22**, 497 (2010).
13. C. Veneault-Fourrey, M. Barooah, M. Egan, G. Wakley, N. J. Talbot, *Science* **312**, 580 (2006).
14. E. Bi *et al.*, *J. Cell Biol.* **142**, 1301 (1998).
15. A. E. Adams, D. I. Johnson, R. M. Longnecker, B. F. Sloat, J. R. Pringle, *J. Cell Biol.* **111**, 131 (1990).
16. I. Sagot, S. K. Klee, D. Pellman, *Nat. Cell Biol.* **4**, 42 (2002).
17. M. Versele, J. Thorner, *J. Cell Biol.* **164**, 701 (2004).
18. L. Li, C. Xue, K. Bruno, M. Nishimura, J. R. Xu, *Mol. Plant Microbe Interact.* **17**, 547 (2004).
19. J. R. Xu, C. J. Staiger, J. E. Hamer, *Proc. Natl. Acad. Sci. U.S.A.* **95**, 12713 (1998).
20. G. Park, C. Xue, L. Zheng, S. Lam, J. R. Xu, *Mol. Plant Microbe Interact.* **15**, 183 (2002).
21. J. Gilden, M. F. Krummel, *Cytoskeleton* **67**, 477 (2010).
22. B. T. Fievet *et al.*, *J. Cell Biol.* **164**, 653 (2004).
23. A. Casamayor, M. Snyder, *Mol. Cell. Biol.* **23**, 2762 (2003).
24. M. Onishi *et al.*, *Mol. Cell. Biol.* **30**, 2057 (2010).
25. M. Iwase *et al.*, *Mol. Biol. Cell* **17**, 1110 (2006).
26. Y. Barral, V. Mermall, M. S. Mooseker, M. Snyder, *Mol. Cell* **5**, 841 (2000).
27. P. A. Takizawa, J. L. DeRisi, J. E. Wilhelm, R. D. Vale, *Science* **290**, 341 (2000).
28. H. Zhao, A. Pykäläinen, P. Lappalainen, *Curr. Opin. Cell Biol.* **23**, 14 (2011).
29. M. J. Egan, Z. Y. Wang, M. A. Jones, N. Smirnoff, N. J. Talbot, *Proc. Natl. Acad. Sci. U.S.A.* **104**, 11772 (2007).
30. P. K. Mattila *et al.*, *J. Cell Biol.* **176**, 953 (2007).
31. T. Takenawa, S. Suetsugu, *Nat. Rev. Mol. Cell Biol.* **8**, 37 (2007).
32. A. Madania *et al.*, *Mol. Biol. Cell* **10**, 3521 (1999).

Acknowledgments: We thank J. Thorner (UC Berkeley) for providing yeast septin mutants, M. Momany for critical reading of the manuscript and valuable discussions, H. Florence from Exeter Mass Spectrometry facility, and M. Schuster from the Exeter Bio-imaging Centre. This work was funded by a Halpin Scholarship for rice blast research to Y.F.D. and grants to N.J.T. from the Biotechnology and Biological Sciences Research Council and the European Research Council. K.Y. is funded by the Kyoto University Foundation. Accession numbers are provided in supplementary materials.

Supplementary Materials

www.sciencemag.org/cgi/content/full/336/6088/1590/DC1
Materials and Methods
Figs. S1 to S12
Tables S1 and S2
References (*33*–*40*)
Movie S1

4 April 2012; accepted 15 May 2012
10.1126/science.1222934

The *lac* Repressor Displays Facilitated Diffusion in Living Cells

Petter Hammar, Prune Leroy, Anel Mahmutovic, Erik G. Marklund, Otto G. Berg, Johan Elf*

Transcription factors (TFs) are proteins that regulate the expression of genes by binding sequence-specific sites on the chromosome. It has been proposed that to find these sites fast and accurately, TFs combine one-dimensional (1D) sliding on DNA with 3D diffusion in the cytoplasm. This facilitated diffusion mechanism has been demonstrated in vitro, but it has not been shown experimentally to be exploited in living cells. We have developed a single-molecule assay that allows us to investigate the sliding process in living bacteria. Here we show that the *lac* repressor slides 45 ± 10 base pairs on chromosomal DNA and that sliding can be obstructed by other DNA-bound proteins near the operator. Furthermore, the repressor frequently (>90%) slides over its natural $lacO_1$ operator several times before binding. This suggests a trade-off between rapid search on nonspecific sequences and fast binding at the specific sequence.

Transcription factors (TFs) have evolved to rapidly find their specific binding sites among millions of nonspecific sites on chromosomal DNA (*1*). In 1970, Riggs *et al.* showed that in vitro the *lac* repressor (LacI) finds its operator apparently faster than the rate limit for three-dimensional (3D) diffusion (*2*). These experiments were explained by the facilitated diffusion theory (*3*, *4*), which posits that TFs search for their binding sites through a combination of 3D diffusion in the cytoplasm and 1D diffusion (sliding) along the DNA. The sliding effectively extends the target region to the sliding distance, which facilitates the search process. Since then, sliding on DNA has been studied in various in vitro assays (*5*–*8*), including direct observations in single-molecule experiments (*9*, *10*). However, the physiological relevance of the long sliding distances observed at low salt concentrations in vitro has been questioned (*11*, *12*). This is because the high intracellular concentrations of salt and nucleoid proteins are expected to reduce sliding distances (*13*). Therefore, whether facilitated diffusion is used in living cells, and if so, how far a TF slides on chromosomal DNA, remain unanswered questions.

Single-molecule imaging provides the time resolution necessary to study TF binding kinetics in living cells. Using a yellow fluorescent protein–labeled LacI in *Escherichia coli* cells, we developed an assay for measuring the search time based on the distinction between localized and diffuse fluorescence signals (*14*). On a 4-s time scale, individual operator-bound LacI-Venus molecules appear as diffraction-limited spots over the background of freely diffusing molecules (Fig. 1A). By measuring the average number of fluorescent spots per cell as a function of time after removing the inducer isopropyl-β-D-1-thiogalactopyranoside (IPTG) (fig. S7), the kinetics of TF binding to an individual operator site in the *E. coli* chromosome can be monitored at a time resolution of seconds (Fig. 1B) (*15*). The fusion to Venus prevents LacI from forming tetramers, thus removing the possibility that the protein will loop DNA. The accuracy of the assay depends on limiting the total number of repressors to three to five molecules per cell (*14*, *16*). This can be achieved (fig. S6) by increasing the autorepression through a single artificial $lacO_{sym}$ operator site partially overlapping the repressor coding region (Fig. 1B, inset).

When we measured the association rate in the strain with a single $lacO_{sym}$ (JE101), we found that it took an average time of 56 ± 2 s (SEM) for any of the three to five fully active (supplementary text) LacI-Venus dimers to bind the operator site (Fig. 1B). This implies that the time required

Department of Cell and Molecular Biology, Science for Life Laboratory, Uppsala University, Sweden.

*To whom correspondence should be addressed. E-mail: johan.elf@icm.uu.se